AD _____

AWB

TECHNICAL REPORT NO. 4

THE PLASTICITY OF NIOBIUM SINGLE CRYSTALS

by

R. Maddin
N.K. Chen

Johns Hopkins

Contract No. Nonr 248(14)
NR 031-383

December 22, 1952

TECHNICAL REPORT NO. 4

THE PLASTICITY OF NIOBIUM SINGLE CRYSTALS

by

R. Maddin
N.K. Chen

Contract No. Nonr 248(14)
NR 031-383

December 22, 1952

TECHNICAL REPORT NO. 4

Contract No. Nonr 248(14)

Studies on the crystallography of the deformation process in body-centered cubic metals have been renewed recently with investigations on the deformation of molybdenum single crystals[1] and of alpha iron single crystals[2, 3, 4]. It is now apparent that too many exceptions to the rationalisation based upon the ratio of absolute testing temperature to absolute melting point temperature by Andrade[5] exist to permit more serious discussion of this type of analysis. The considerations of resolved shear stress utilising only planes of a type $\{110\}$, $\{112\}$ and $\{123\}$ [6, 3] permit analysis of the deformation only on the basis of these three type planes.

The suggestions made by Chen and Maddin[1] in which the slip process is envisioned as a composite slip on two non-parallel $\{110\}$ planes (this suggestion was made earlier by C. F. Elam[7] and by A. B. Greninger[8]) can be illustrated schematically in Fig. 1. It may be seen that an unresolved trace on any plane containing a $\langle 111 \rangle$ direction may be accomplished by varying the number of atoms participating in the composite process. By further varying the number of atoms in each plane but keeping the ratio of the participating atoms constant, one could then ob-

tain jogs in the traces and hence produce wavy slip lines. Evidence for the composite nature of the process has been presented for the case of molybdenum in the form of analysis of asterism and longitudinal axis migration. Further evidence on molybdenum in the case of bending and by use of x-ray microscopy will be forthcoming shortly in other publications.

Vogel and Brick[2] have studied the behavior of alpha iron crystals in which they suggest that the plane of glide is non-crystallographic and may be predicted from the intersection between the great circle joining the slip direction and specimen axis with the great circle whose zone axis is the slip direction. However, the asterism developed in their investigation was not sufficient to permit analysis in the same manner as used by Chen and Maddin. Consequently, only the unresolved traces were considered in their analysis.

The present investigation was attempted in order to study the behavior of niobium single crystals, not only in tension but also in compression since the specimen axis migration should indicate the plane or planes of glide in the same manner that the specimen axis migration in tension indicates the direction of glide.

Experimental Procedure

Single crystals of niobium approximately 3 mm. in diameter varying in length were grown by the method previously described for molybdenum[9]. It was not always possible to obtain very long single crystals and quite often more than one large grain occupying the total cross-section was present in the extension specimens. For the compression specimens, it was a simple matter to cut crystals of proper length to permit accurate studies of the deformation process.

Surface preparations were very difficult since a good electrolytic polishing solution was not available to insure proper surface conditions for micrographic work. A solution suggested by G. W. Wensch[10] consisting of 85% concentrated sulphuric acid, 15% concentrated hydrofluoric acid, was used with a platinum cathode, a current density of 0.04 amperes per square centimeter, and a temperature between 25 and 60°C with a limited amount of success. Consequently, the micrographs reproduced here leave something to be desired.

Experimental Results

The initial orientations of all crystals investigated are shown in Fig. 2. Although nine crystals were deformed, orientations in the vicinity of the (001) were not available in order to consider the effect of orientation on the crystallography of deformation. In terms of the Opinsky and Smoluchowski plot of planes of maximum resolved shear stress, however, there are crystals whose orientations fall within the area where one of each type of plane, i.e., $\{110\}$, $\{112\}$, and $\{123\}$ would have the highest resolved shear stress.

Crystal No. 2 was approximately two centimeters long and occupied the entire cross-section of the 3 mm. rod. The rod was pulled in a hydraulic tensile machine to the first appearance of slip lines. Laue back reflection photograms showed a longitudinal axis shift towards the $[\bar{1}11]$ (direction C). Stereographic analysis of the slip traces at every 10 degrees in azimuth around the specimen gave a non-crystallographic plane as the plane of glide. Longitudinal axis shift and the pole of the plane determined from slip plane traces are shown in Fig. 3. Unfortunately, the surface of the crystal was quite smudged and observations of

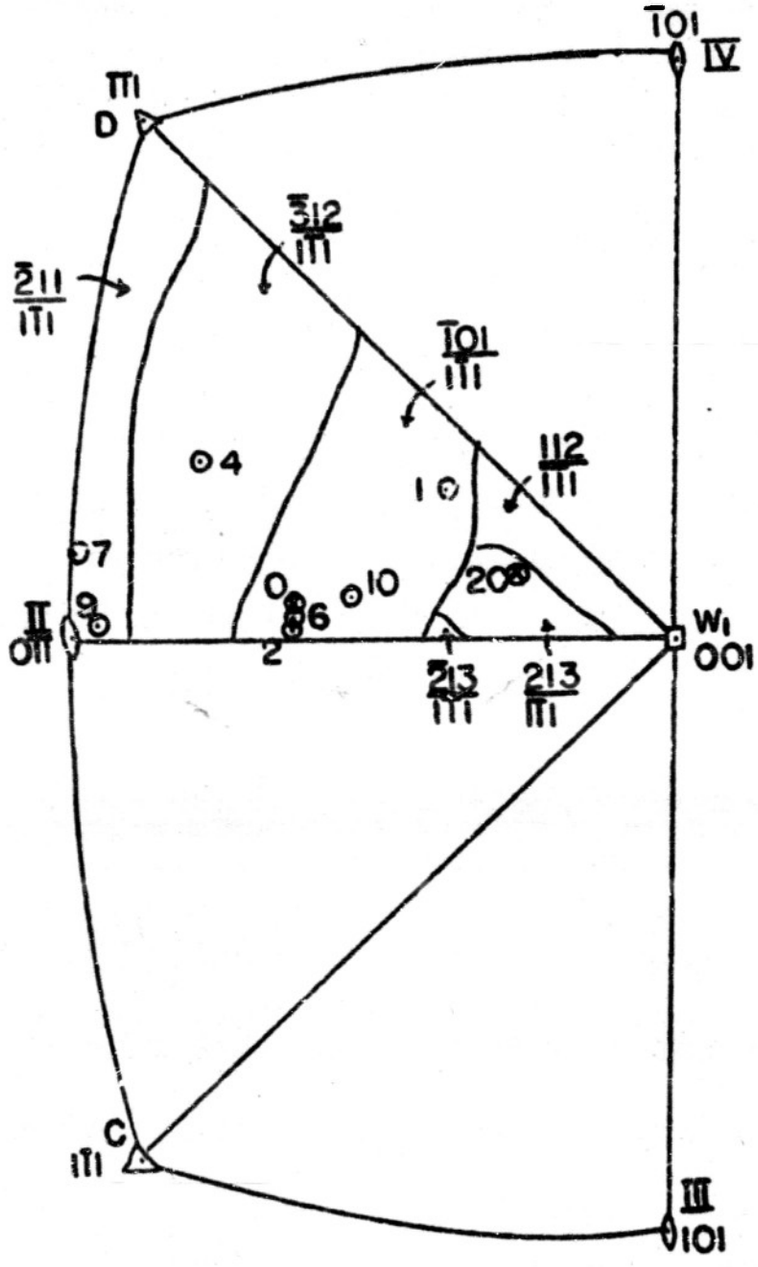

Fig. 2 - Initial Orientations of All Crystals Investigated. Triangle Is Divided into Areas Indicating the Slip Systems of Highest Resolved Shear Stress (with Reference Only to $\{110\}$, $\{112\}$, and $\{123\}$ Planes).

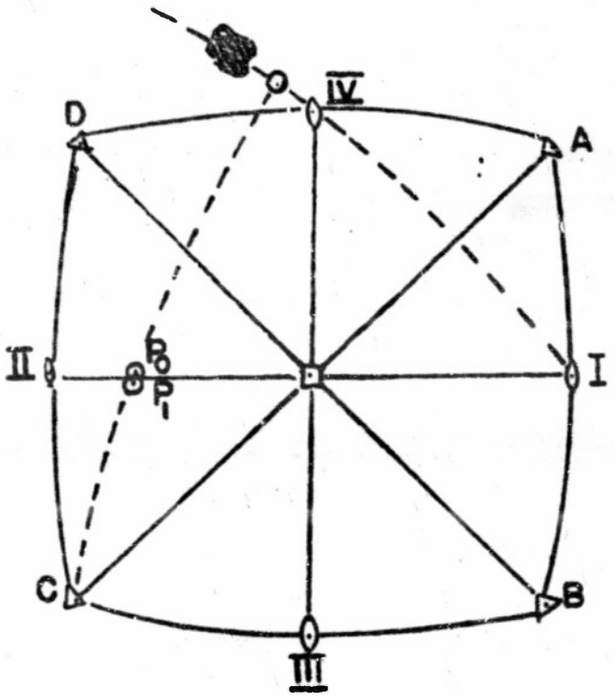

Fig. 3 - Initial and Final Orientation of Crystal Nb-2. Stereographic Determination of Traces Shown as Solid Area. Glide Plane Pole Predicted by Intersection Method Shown as Unmarked Circle[2].

the traces were difficult. Little asterism was present after this small deformation and analysis of the planes of glide based upon asterism could not be made.

Crystal Nb-4, approximately the same length as Nb-2, was extended three per cent in the first elongation. Although stereographic analysis of the traces observed indicated a non-crystallographic plane of slip, analysis of the asterism indicated the $(0\bar{1}1)$ and the $(\bar{1}01)$ as the planes of glide (planes II and IV in Fig. 4). This may be seen in Fig. 4 where the longitudinal axis shift is plotted together with the asterism shown in Fig. 5(a) as P_0 and P_1. From the longitudinal axis shift plotted using the tails of the asterism, it may be seen that the activity of two planes has occurred. In an effort to determine more accurately the axis about which asterism occurred, Laue back reflection photograms were made every two degrees about the specimen axis in the vicinity of the critical position. The photogram shown in Fig. 5(b) clearly demonstrates a $[\bar{1}\bar{1}2]$ axis as that about which asterism occurred. The photogram was plotted stereographically in order to indicate the plane and direction of glide. This plot again showed the $(0\bar{1}\bar{1})$ $[\bar{1}11]$ (IIA) to be one of the slip systems acting.

This crystal was extended again until necking occurred. Laue photograms were made in the section adjacent to the necked region. The final position of the longitudinal axis is shown labeled as P_2 in Fig. 4. It is clearly demonstrated that the predominant system is $(\bar{1}01)$ $[1\bar{1}1]$ (IVC) accounting for the axis shift from P_1 to P_2. Collateral gliding on the other system $(0\bar{1}\bar{1})$ $[\bar{1}11]$ (IIA) was suspected from the photograms but asterism was too great to permit a careful analysis.

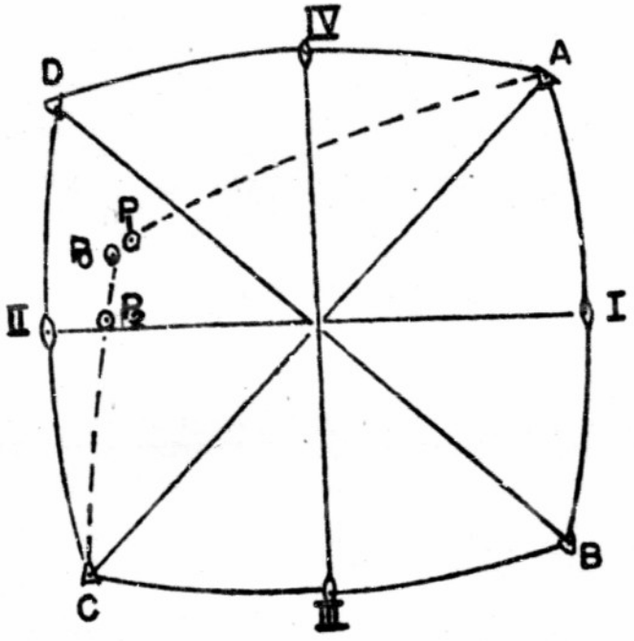

Fig. 4 - Initial and Final Orientation of Crystal Nb-4.
P_0-P_1 Indicate Positions of Asterism End Points.

Crystal Nb-7 was pulled until necking occurred in the grain. Laue photograms did not permit analysis of the extreme asterism but did permit a plot of the axis shift. It should be pointed out that the final longitudinal axis position, P_1, was determined by noting only one point (that of maximum density) on extensive streaks. This is shown in Fig. 6. Although a rotation towards the $[111]$(B) can be noted, little can be said regarding the plane of glide except that were the system of maximum shear stress to have operated, the axis shift would have been towards the $[1\bar{1}1]$(C). This activity in Nb-7 points to the complexity of the deformation in the body-centered cubic crystals.

Crystal Nb-6 was extended approximately five per cent. Surface conditions were better here and stereographic analysis of these traces, shown in Fig. 7, gave the $(\bar{1}01)$ as the plane of glide. In this case, the axis shift, shown in Fig. 8, indicated the slip system to be $(\bar{1}01)$ $[1\bar{1}1]$ (IV-C). The method of analysis for ferrite single crystals used by Vogel and Brick[2], where a great circle drawn through the axis of the specimen and the slip direction intersects the great circle whose pole is $[1\bar{1}1]$, designates the plane of glide to be very close to $(\bar{1}01)$. The asterism in the Laue photograms was complex but not enough developed to permit accurate plotting. There was present in the complexity, however, the indication that $(\bar{1}01)$ $[1\bar{1}1]$ (IV-C) was not the only slip system.

The behavior of crystal Nb-9 was quite complex. The initial orientation, Fig. 9, was very close to the $(0\bar{1}\bar{1})$ and very close to the $(0\bar{1}\bar{1})$-(001) boundary. Two flat surfaces at 90° angles were polished on the specimen held in sealing wax. After etching in concentrated HF, the specimen was electropolished. Laue back reflection photograms were made

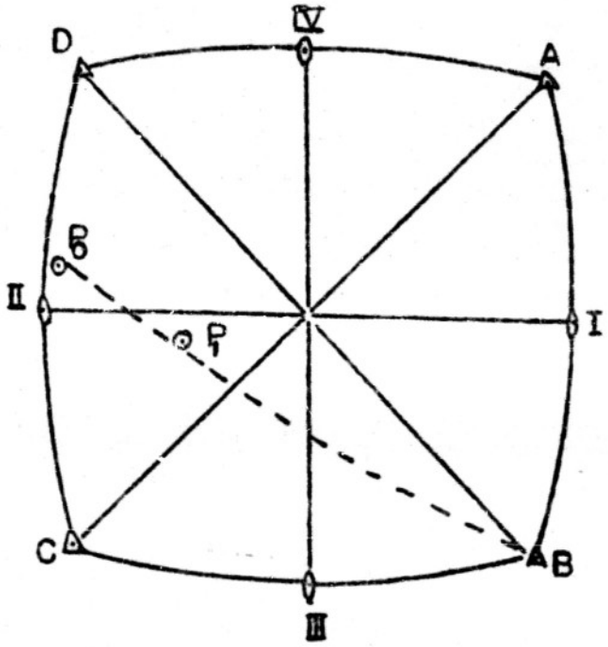

Fig. 6 - Initial and Final Orientation of Crystal No-6.

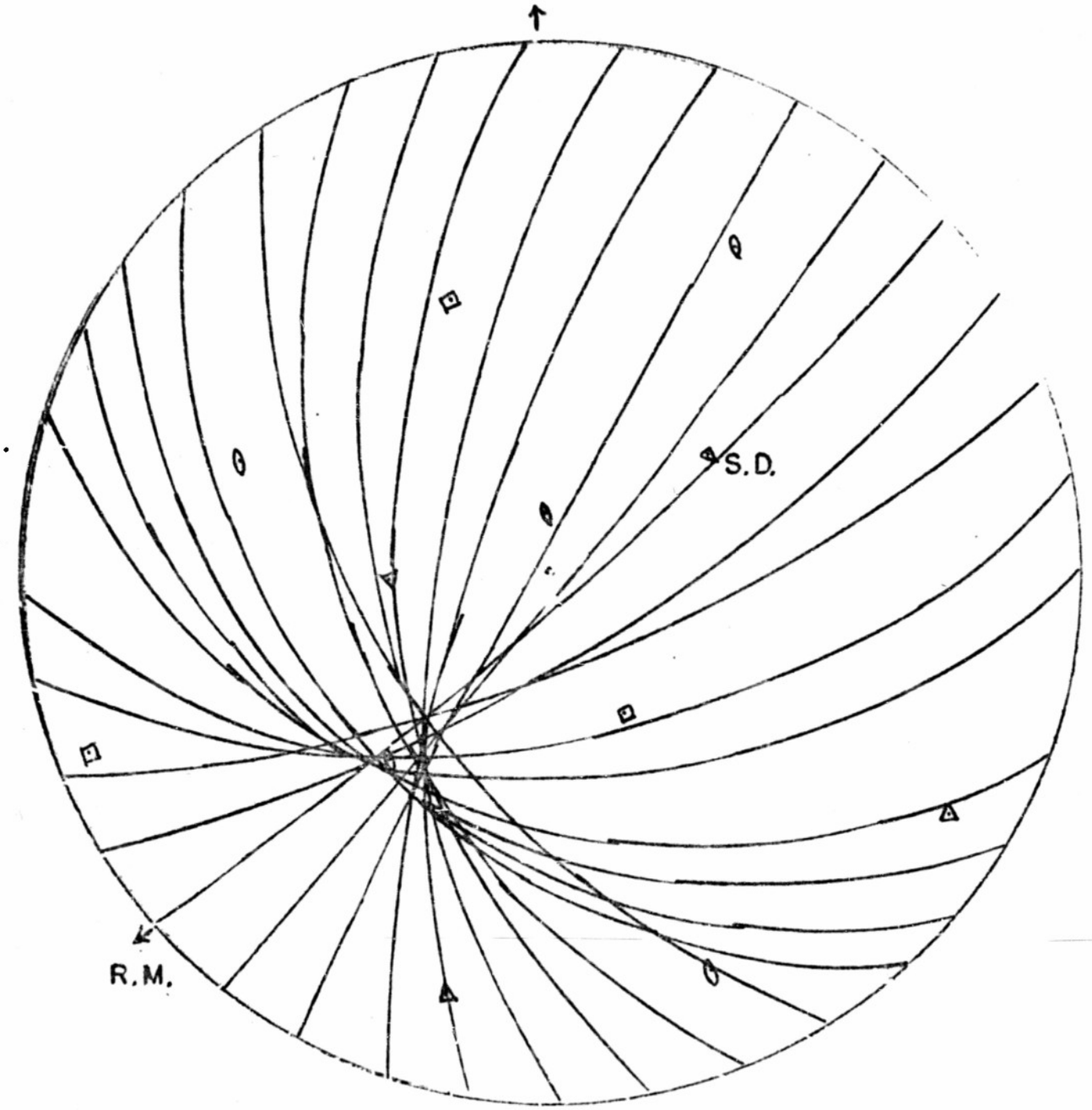

Fig. 7 - Stereographic Plot of Slip Traces at Every 10 Degrees in Azimuth. Area Enclosed (101) Pole. Crystal Nb-7.

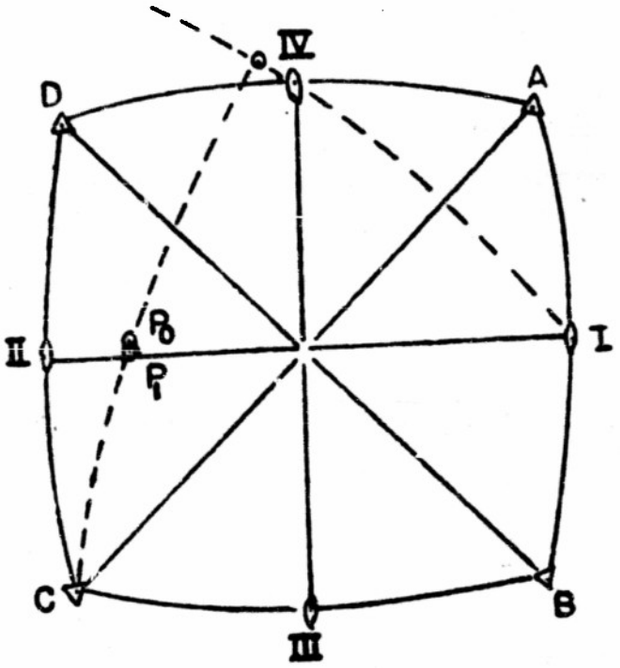

Fig. 8 - Initial and Final Orientation of Crystal Nb-7.
Predicted Pole Shown as Unmarked Circle.

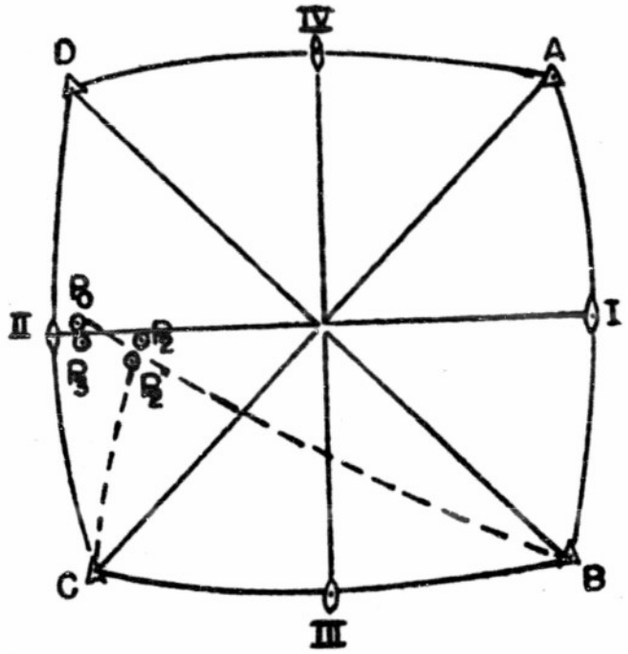

Fig. 9 - Initial, Intermediate and Final Orientation of Crystal Nb-9. P_2-P_2^1 Designate End Points of Asterism.

of each surface to indicate the removal of material affected by the polishing.

The specimen was extended about two per cent and examined with microscope and x-rays. No slip lines could be observed and little or no axis shift could be observed. The specimen was extended again to a total elongation of about six per cent. Although slip lines were visible, great difficulty was encountered in attempting analysis from the traces. X-ray photograms made at different positions around the specimen axis testified to the complex behavior of this crystal. Referring to Fig. 9, the initial orientation of the crystal is plotted as P_0 and the position of the axis after six per cent elongation by P_2. The axis shift indicates a rotation towards [111] (B), the possible slip direction. The system II-B, however, is one of very low shear stress. Consequently, the action may be of a composite nature involving the planes IV and V (not shown here), both containing the direction B. In view of the fact that a plot of the extent of asterism shows the participation of system IV-C, it might be suggested that in addition to the activity of planes IV and V in direction B, there is the participation of IV in direction C. After extension again to about 16 per cent, the position of the axis was at P_3, Fig. 9. The behavior of Nb-9 after 16 per cent elongation might now be explained by the participation of slip systems III-D and IV-C. Again, the slip lines were extremely complex showing not only very wavy nature but also the pronounced development of deformation bands.

The behavior of Nb-10 with an initial orientation almost the same as Nb-9 but farther along the symmetry curve $(0\bar{1}1)$-(001) was not quite so complex. After about six per cent elongation, the axis shift, P_0 to P_1 in

in Fig. 10, might likewise be explained on the participation of systems IV and V in direction B. However, after 16 per cent elongation the axis shift indicated a participation of $(0\bar{1}1)\,[\bar{1}11]$ (II-A). The small deviation along the great circle to $[\bar{1}11]$ (B) may perhaps be attributed to the continual participation of IV and V in Direction B, but on a small scale. However, the position of P_3, being at the outer limit of the accuracy of orientation determination, cannot be classed as rigorously indicating the later activity of $(0\bar{1}1)\,[\bar{1}11]$ (II-B).

The behavior of Nb-1, extended about five per cent, could be called classical. The analysis of the slip traces showed $(\bar{1}01)$(IV) to be the plane of glide and the axis shift is primarily towards the proper $[1\bar{1}1]$ (C) (Fig. 11). Little can be said here about the collateral participation of other $\{110\}$ planes since little asterism was present after this extension.

Nb-0 was approximately 10 mm. long by 3 mm. in diameter. Its ends were milled and ground parallel. Following this operation, the specimen was polished electrolytically and compressed with a special jig in a hydraulic compression machine; the bearing compression plates were greased and the load was applied carefully. The first compression amounted to 5.97 per cent. Confirmation of $(\bar{1}01)$ as the plane of glide was obtained from analysis of the traces stereographically.

The appearance of slip traces on Nb-0 after the first compression is shown in Fig. 12 (a-d). The traces are, for the most part, straight and prove to be caused by the $(\bar{1}01)$ plane. The forked bands are presumably deformation bands whose boundaries agree with no low indices, high atomic density plane. In certain cases, the bands are seen to consist of

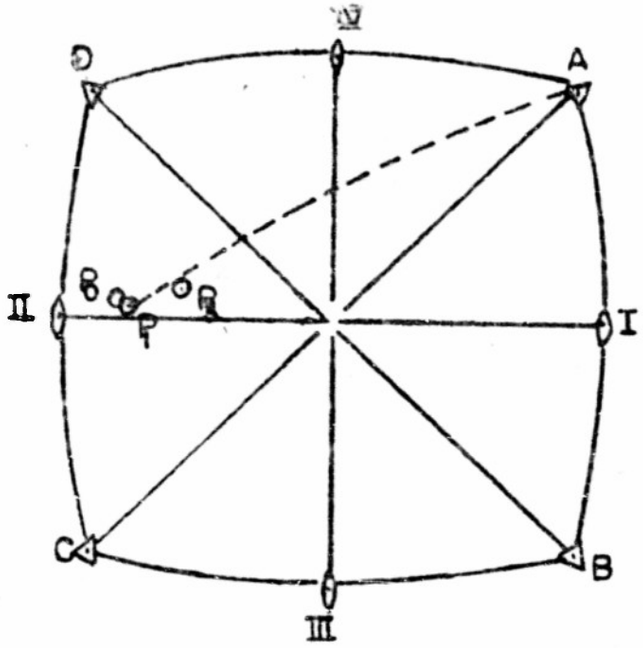

Fig. 10 - Initial, Intermediate and Final Orientation of Crystal Nb-10.

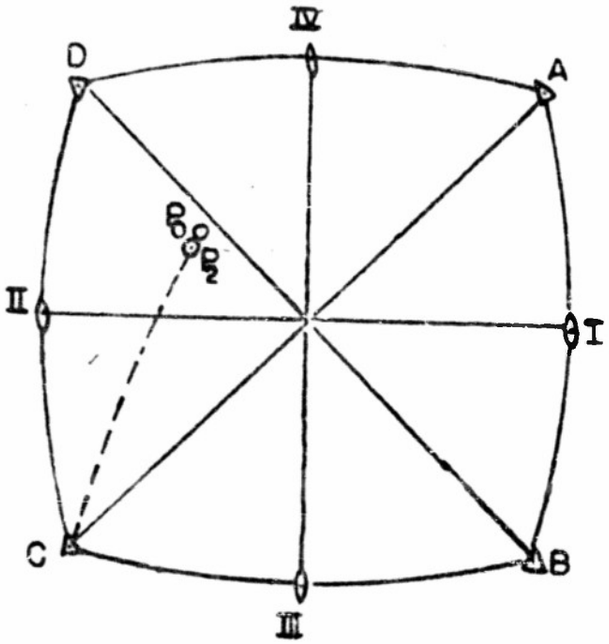

Fig. 11 - Initial and Final Orientation of Crystal Nb-11.

small but straight lines reminiscent of bands of secondary slip in aluminum.

The behavior of metal single crystals in compression has been investigated frequently in order to determine the plane of glide. Just as the change in position of the longitudinal axis after extension indicates the glide direction, the same change in axes after compression indicates the pole of the plane of glide when glide occurs completely or predominantly on a series of parallel planes.

Reference to Fig. 13 in which P_0 migrates to P_1 can be explained from the activity of slip systems $(\bar{1}01)\ [1\bar{1}1]$ (IV-C) and $(101)\ [\bar{1}\bar{1}1]$ (III-D). Further evidence can be cited from the behavior of this specimen after compression to 11 per cent. The x-ray photogram shown in Fig. 14 is seen to consist of two distinguishable asterisms. If the tails of these are plotted separately, indicated as P_1-P_2 and P_1-P_2', a clear participation of the slip system IV-C and III-D may be noted.

In an attempt to consider more carefully the extent of disorientation existing in the surface layers of the specimen after deformation, x-ray microscopy [10, 11] was used. $Cu\ K_\alpha$ radiation, 30KV, was reflected from a bent quartz crystal monochromator and focused on the specimen supported on a two circle goniometer. Reflections were obtained for certain specimen positions and recorded on spectroscopic VO plate held parallel to the focused beam almost tangent to the specimen surface yielding the reflection. Exposures of from one-half to four hours were necessary to obtain suitable records. In Fig. 15 (a, b, c) there is shown the striated and banded structure observed by this technique. The amount of disorientation as a result of 5.47 and 11 per cent compression can be seen, at least qualitatively in these x-ray micrograms.

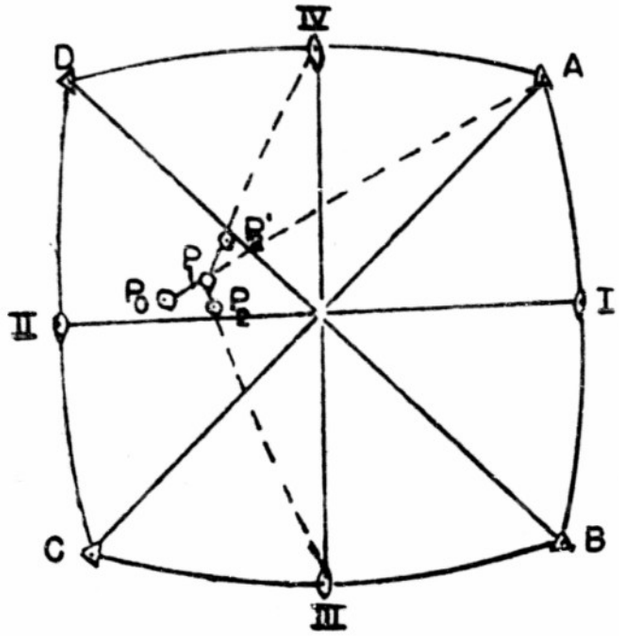

Fig. 13 - Initial and Final Orientations of Crystal Nb-o (Compression). P_2-P_2^1 Indicate End Points of Double Asterisms Shown in Fig. 14.

Throughout these compression studies, it was apparent that the amount of distortion (asterism) produced per amount of deformation is far greater in the case of compression than in tension. For example, after 16 per cent compression, the asterism is so great as not to permit orientation determinations whereas the same amount of extension produces much less disorientation.

Specimen Nb-2c was treated in the same manner as Nb-0. It was compressed 2.91 per cent and observed by microscope, x-ray and x-ray microscopy. Analysis of the traces indicated three glide planes to have been operative; these were $(\bar{1}10)$ (VI), $(0\bar{1}1)$ (II), and (101) (III). A micrograph of three sets of traces is shown in Fig. 16. It is possible that the slip direction is the same for all three of these planes. If the amount of glide on each of these planes in the same slip direction is the same, the movement of the axis along a great circle to (101) would be expected. However, as may be seen in Fig. 17, the pole movement P_0 to P_1 is not exactly along this great circle indicating an uneven amount of glide on the $\{110\}$ planes concerned. After 14.5 per cent compression, however, it is apparent that the glide on the plane (101) (III) predominates as shown by the movement of P_1 to P_2.

Discussion of Results

Determination of glide planes from observation of the traces on the surface might be questionable when these traces are wavy, branched and forked. Such is normally the case with traces observed on plastically deformed body-centered cubic crystals. Nevertheless, a direction is generally assigned to a wavy trace and with many such observations, a determination of the apparent glide plane may be made. Such an example is seen in

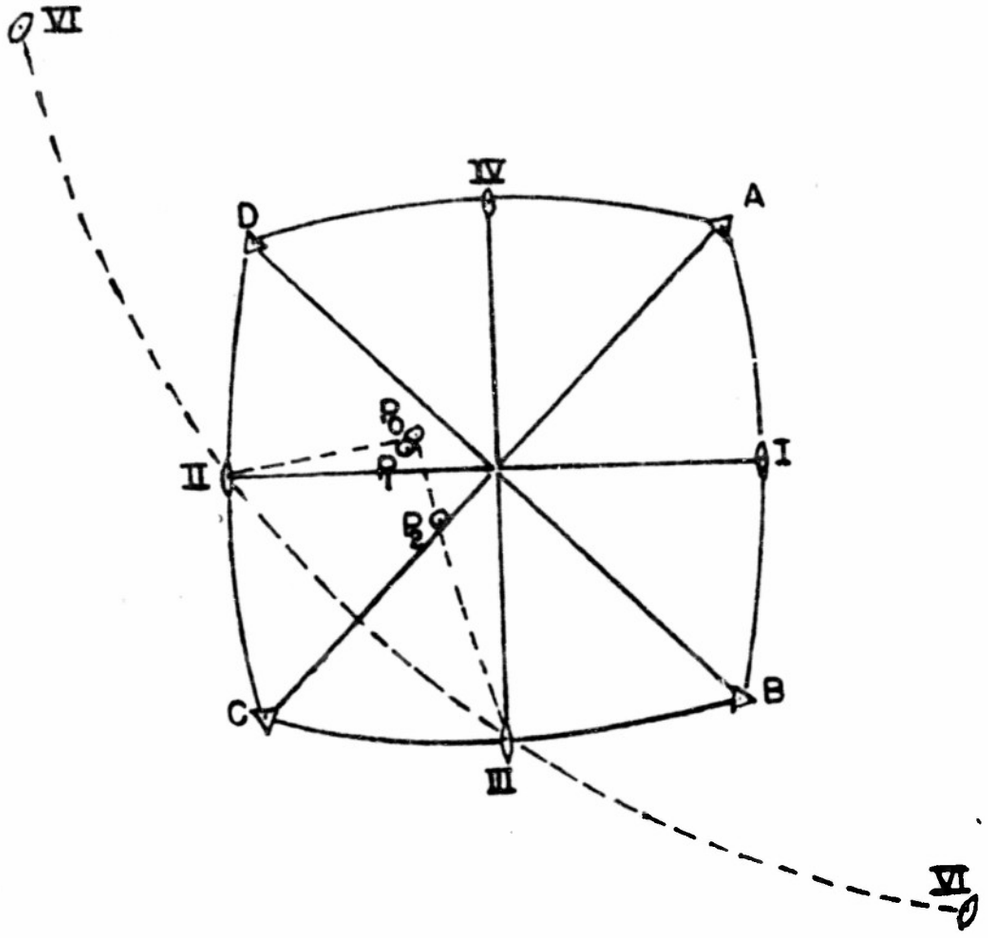

Fig. 17 - Initial, Intermediate, and Final Orientation of Crystal Nb-2C (Compression).

Fig. 7. Here, the amount of extension was about 5 per cent and with this small deformation, the traces appeared somewhat straight.

With compression of niobium, however, the deformation markings are of a different character. Two types can be noted, (c.f. Fig. 12, 16) those lines which are straight and narrow wherever observed and those bands of relatively large width which are branched, forked and wavy. Stereographic plots of the straight narrow lines show $\{110\}$ to be the glide plane whereas similar plots of the bands yield no confirmation. It is also possible to observe very small straight, narrow segments composing the bands; these, too, apparently prove to be caused by $\{110\}$ planes.

Perhaps a more sensitive indication of the glide plane would be found in analysis of the asterism resulting from deformation. As in the case of molybdenum[1], a $\langle 112 \rangle$ axis is shown to be the axis about which asterism occurs. In the case here reported (Fig. 4b), it is readily seen that this axis is $[121]$ in which case the plane of glide is $(\bar{1}01)$ and the direction $[1\bar{1}1]$ if it can be assumed that plastic deformation in the body-centered cubic crystals, i.e. rotation of the plane of glide is about an axis in the plane and normal to the direction of glide. There appears to be sufficient observations to support this assumption in the body-centered cubic crystals[13, 14]. Had other type planes acted as glide planes, other axes should be observed as the axes about which rotation occurs, e.g. for a $\{112\}$ a $\langle 110 \rangle$ would operate. However, these have not been observed to date.

The optical analogy between diffraction of x-rays by bent atomic planes and the reflection of light by curved mirrors provides the basis for a method for interpreting asterism from deformed single crystals at

least qualitatively in terms of the direction of rotation of the atomic planes[15]. Thus, if the ends of the asterism are plotted stereographically, the direction of displacement of these asterisms interpreted as positions of the longitudinal axis of the specimen indicates the direction of glide in tension and the plane of glide in compression. For example, the extent of asterism in Fig. 4 indicates the participation of slip system II-A in the first extension. Later rotation, however, shows the operation of system IV-C. It would appear that the correct interpretation is that where both systems operate. A similar example may be seen in Fig. 9. In the compression case, Fig. 13, a more apparent activity presents itself. Here, the rotation independent of asterism is not directly conclusive of any particular plane of glide, whereas the extent of asterism clearly demonstrates the collateral operation of IV-C and its conjugate II-A. A somewhat similar example is seen in Fig. 17 where one $\{110\}$ plane has acted predominantly in the later stages of deformation as indicated by the large rotation towards this pole.

The use of x-ray microscopy lends further support to the idea that slip in the body-centered cubic crystals occurs in a composite fashion. Although the resolution derived by this method is not greater than what is generally attainable with light microscopy, effects of surface conditions can be eliminated. Thus if there existed a sudden change in direction of slip traces which could not readily be observed because of surface conditions, x-ray microscopy might be expected to showthis. Examples of this effect have been found in extended molybdenum single crystals[16]. Examples in Fig. 15 show relatively straight striae and bands where optical microscopy reveals branched and wavy bands.

The question may well be asked as to why planes of lower resolved shear stress but of high atomic density would act in contrast to lower atomic density planes with higher resolved shear stress. C. H. Mathewson[17] has provided a possible answer to this. Consider the schematic drawing in Fib. 18(a) which shows the relation between a (112) plane of high resolved shear stress, a composite (112) plane constructed of non-parallel $\{110\}$ planes for the orientation where the (112) planes would be predicted on the basis of resolved shear stress (Nb-7 or Nb-9 in Fig. 1). The area of the composite plane constructed from two non-parallel $\{110\}$ planes is

$$\frac{S_{112}}{\cos 30^\circ} = 1.15\, S_{112}$$

Similarly, Fig. 18(b) shows the same relation between a (123) plane and a composite (123) plane constructed by using a ratio of three atoms of one $\{110\}$ to one of another non-parallel $\{110\}$. Here the area of the composite is obtained from trigonometric relations to be

$$\frac{S_{123}}{0.883} = S_{123} \times 1.133$$

Since the $\sin\chi \cos\lambda$ factor is the same in both cases if the assumption of composite slip is made, the resolved shear stress is only 15 per cent greater on the pseudo (112) plane and only 13.3 per cent greater on the pseudo (123) plane. It would appear that a mathematical basis for composite slip might exist.

The problem of resolving the traces into their composite nature would best be solved with aid of the electron microscope provided the actual number of atoms participating in the process is sufficiently large (the ratio remaining constant). Attempts are now being made using extended

molybdenum single crystals.

A second possibility of presenting good evidence in favor of composite slip would be to develop a sensitive load measuring device in order to distinguish the small differences in load resolved along actual and "pseudo" planes. Careful resolved shear stress measurements would indicate the plane or planes along which glide has occurred. These experiments are now being contemplated using single crystals of various body-centered cubic metals.

Acknowledgment

The authors would like to take this opportunity to acknowledge with appreciation the many helpful discussions of Dr. C. H.Mathewson and for application of the idea of composite slip to the present analysis.

References

(1) N. K. Chen and R. Maddin: "Plasticity of Molybdenum Single Crystals," Jnl. Metals, Oct. 1951

(2) F. L. Vogel and R. M. Brick: "Deformation of Ferrite Single Crystals," Technical Report No. 1; July 1, 1952, Contract AF 33-(038)15889, Univ. of Penn., Phila., Pa.

(3) A. J. Opinsky and R. Smoluchowski: "Crystallographic Aspect of Slip in Body-Centered Cubic Crystals," Symposium, Carnegie Inst. Tech., May 1950

(4) A. J. Opinsky and R. Smoluchowski: "The Crystallographic Aspect of Slip in Body-Centered Cubic Single Crystals," Jnl. of Appl. Physics, 22, (1950), 1488

(5) E. N. daC. Andrade: Report of a Conference on Internal Strains in Solids, Proc. Phys. Soc., London, 52, (1940), 1

(6) N. Farhenhorst and E. Schmid: Z. Physik, 78, (1932), 383

(7) C. F. Elam: "The Distortion of Metals," (1935), Oxford, Clarendon Press

(8) A.B. Greninger: Discussion to C.S. Barrett, G. Ansel and R. F. Mehl: "Slip, Twinning and Cleavage in Iron and Silicon Ferrite," Trans. ASM, 25, (1937) 702

(9) N. K. Chen, R.Maddin and R. B. Pond: "Growth of Molybdenum Single Crystals," Jnl. Metals, June 1951, 461

(10) G. W. Wensch: Private Communication

(11) W. Berg: "Load History of Deformed Crystals," Zeits Krst, 89, (1934), 286

(12) C. S. Barrett: "A New Microscopy and Its Potentialities," Trans. AIME, (161),(1945), 15

(13) E. N. daC. Andrade and L. C. Tsien: "Glide of Single Crystals of Sodium and Potassium," Proc. Roy. Soc., London, A163, (1937), 1

(14) C. S. Barrett: "Structure of Metals," 2nd Edition, McGraw-Hill, N. Y., p. 375

(15) Ibid, p. 414-420

(16) N. K. Chen and R.Maddin: "Glide in Extended Molybdenum Single Crystals," to be submitted for publication

(17) C. H. Mathewson: Private communication

PLATE I

Fig. 1. Illustration Showing the Integrated Trace Produced by Using Different Numbers of Atoms in Non-parallel $\{110\}$ Planes.

Fig. 5. X-ray Photograms of Crystal Nb-4.
(a) This Shows Two Distinct Asterisms. The Larger of the Two Is Plotted Stereographically in Fig. 4.
(b) Photogram Used for Determining Axis of Asterism.

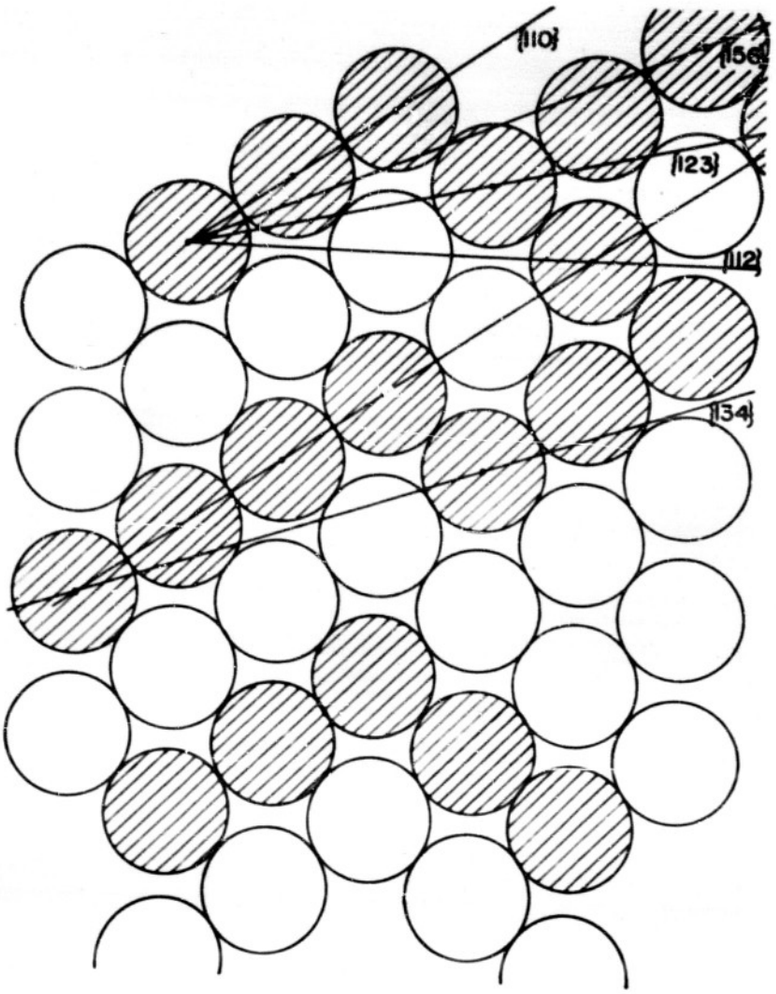

Fig. 1

A B

Fig. 5

PLATE II

Fig. 12. Slip Lines and Deformation Bands in Crystal Nb-O (Compression)

(b) Rotated 58 Degrees from Position (a)
(c) Rotated 160 Degrees from Position (a)
(d) Rotated 20 Degrees from Position (a)

Fig. 14. X-ray Photogram Showing Two Asterisms. These Are Plotted in Fig. 13 as P_2-P_2^1.

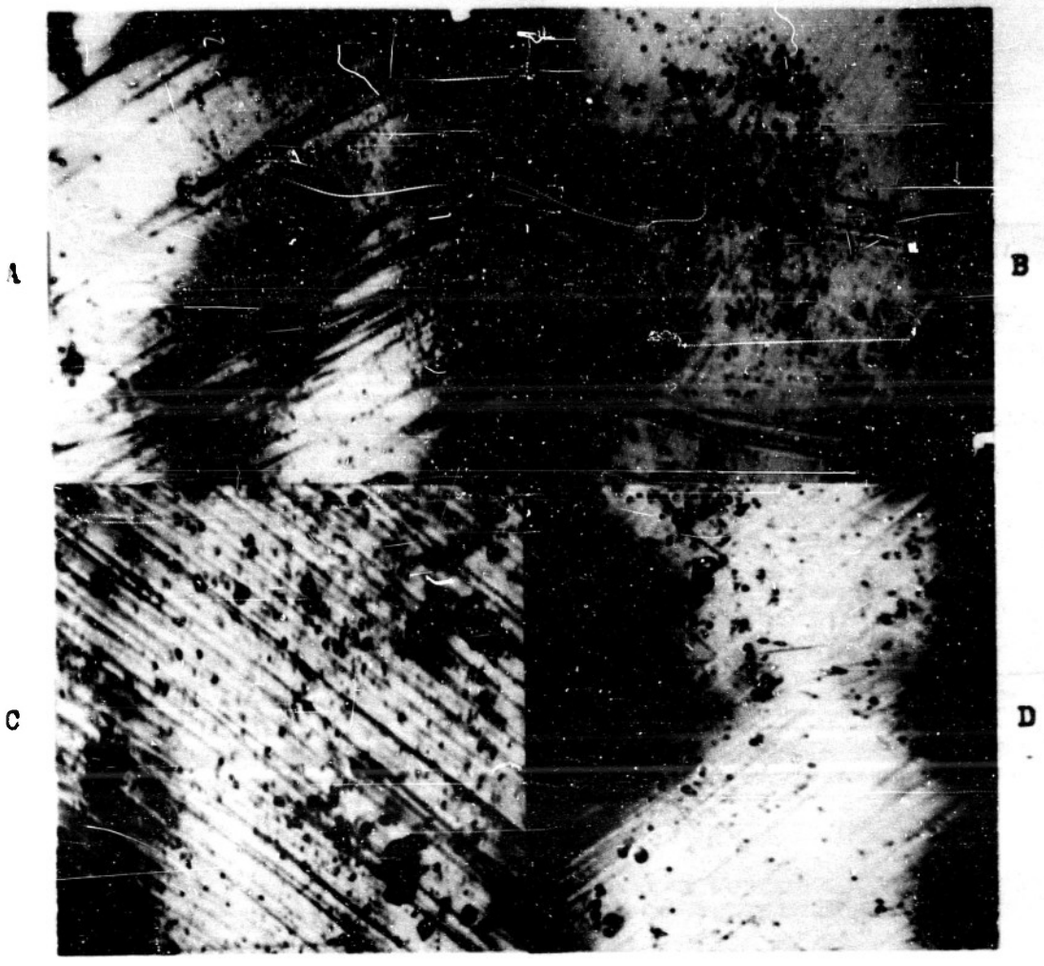

Fig. 12

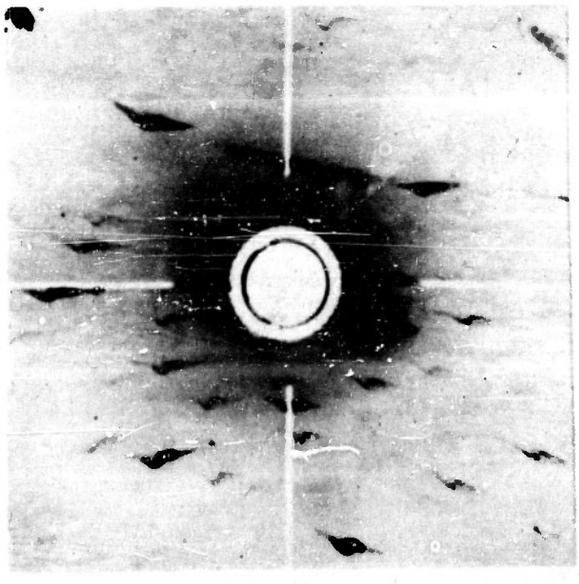

Fig. 14

PLATE III

Fig. 15. X-ray Micrograms of Crystal Nb-o Made Using Bent Quartz Monochromator; 30 Kv Cu K_{α} Radiation V-O Plate.
(a) Nb-o After First Compression. X70
(b) Nb-o After First Compression from Another Set of Planes. X70
(c) Nb-O After Second Compression. X110

Fig. 16. Three Sets of Slip Lines in Compression Specimen Nb-2C.

Fig. 18 (a). (112) Plane as Compared with "Pseudo" (112) Plane Made by Using Equal Numbers of Atoms in Two Non-parallel {110} Planes.

Fig. 18 (b). (123) Plane as Compared with "Pseudo" (123) Plane Made by Using Three Atoms of One {110} Plane and One Atom of a Non-parallel {110} Plane.

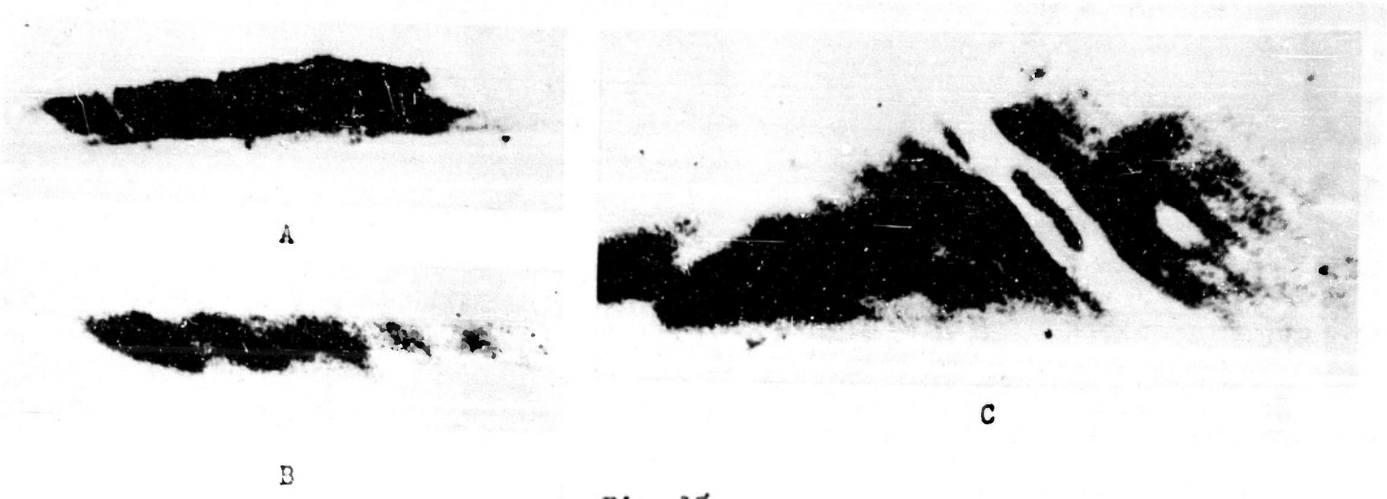

A

B

C

Fig. 15

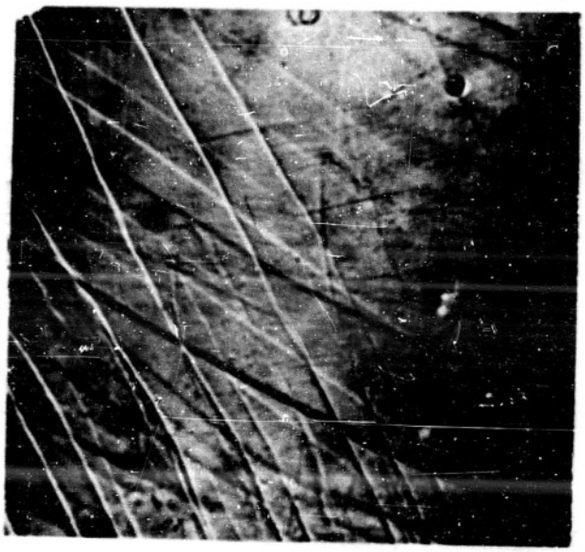

Fig. 16

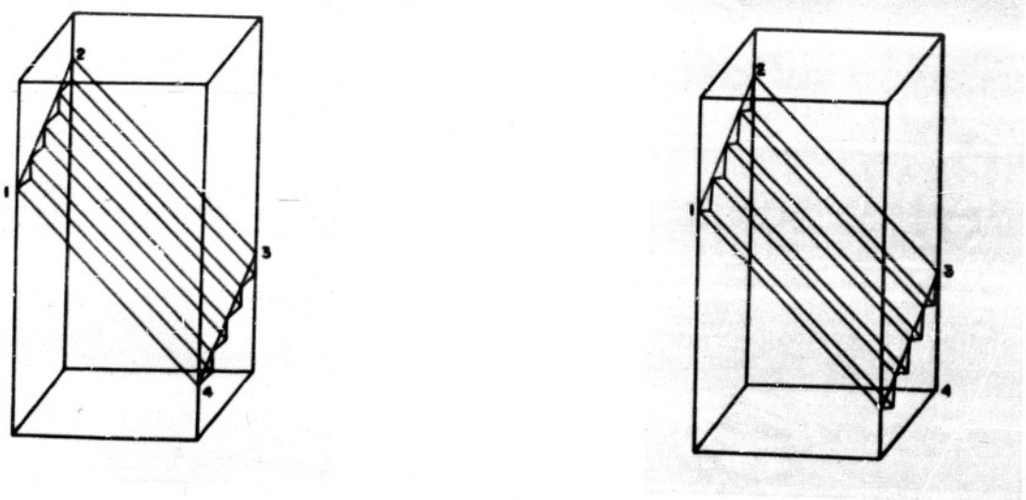

A

Fig. 18

B

DISTRIBUTION LIST

For -
Technical and Summary
Reports on Contract No. Nonr 248 (14)

NAVY

Chief of Naval Research
Department of the Navy
Washington 25, D. C.
Attn: Code 423 (2)

Commanding Officer
Office of Naval Research
Branch Office
495 Summer Street
Boston 10, Massachusetts (1)

Commanding Officer
Office of Naval Research
Branch Office
50 Church Street
New York 7, New York (1)

Commanding Officer
Office of Naval Research
Branch Office
801 Donahue Street
SanFrancisco 24, Cal. (1)

Commanding Officer
Office of Naval Research
Branch Office
844 N. Rush Street
Chicago 11, Illinois (1)

Commanding Officer
Office of Naval Research
Branch Office
1030 Green Street
Pasadena, Cal. (1)

Assistant Naval Attache for
Research, London
U. S. Navy
FPO 100
New York, New York (5)

Contract Administrator,
SE Area
Office of Naval Research
Department of the Navy
Washington 25, D. C.
Attn: Mr. R. F. Lynch (1)

Director, Naval Research Laboratory
Washington 25, D. C.
Attn: Technical Information Officer (1)

Director, Naval Research Laboratory
Washington 25, D. C.
Attn: Code 3500, Metallurgy Division (1)
Code 2020, Technical Library (1)

Bureau of Aeronautics
Navy Department
Washington 25, D. C. (3)
Attn: N. E. Promisel, AE-41
Technical Library, TD-41 (1)

Commanding Officer
Naval Air Material Center
Naval Base Station
Philadelphia, Pennsylvania
Attn: Aeronautical Materials Lab. (1)

Bureau of Ordnance
Navy Department
Washington 25, D. C.
Attn: Rex (3)
Technical Library, Ad3 (1)

Superintendent, Naval Gun Factory
Washington 20, D. C.
Attn: Metallurgical Laboratory,
In910 (1)

Commanding Officer
U. S. Naval Ordnance Laboratory
White Oaks, Maryland (1)

Commanding Officer
U. S. Naval Ordnance Test Station
Inyokern, California (1)

Bureau of Ships
Navy Department
Washington 25, D. C.
Attn: Code 343 (5)
Code 337L, Technical Library (1)

NAVY

U. S. Naval Engineering Experiment Station
Annapolis, Maryland
Attn: Metals Laboratory (1)

Director Materials Laboratory
Building 291
New York Naval Shipyard
Brooklyn, New York
Attn: Code 907 (1)

Chief, Bureau of Yards and Docks
Navy Department
Washington 25, D. C.
Attn: Research and Standards Div. (1)

Bureau of Ordnance
Department of Navy
Washington 25, D. C.
Attn: F. J. Perella (Re9A) (1)

Bureau of Ships
Department of the Navy
Washington 25, D. C.
Attn: Code 390 (1)

ARMY

Chief of Staff, Department of Army
The Pentagon
Washington 25, D. C.
Attn: Director of Research and Development (1)

Office of the Chief of Ordnance
Research & Development Service
Department of the Army
The Pentagon
Washington 25, D. C.
Attn: ORDTB-Research Coordination Branch (3)

Commanding Officer
Watertown Arsenal
Watertown, Massachusetts
Attn: Laboratory Division (1)

Commanding Officer
Frankford Arsenal
Philadelphia, Pennsylvania
Attn: Laboratory Division (1)

Office of the Chief of Engineers
Department of the Army
The Pentagon
Washington 25, D. C.
Attn: Research and Development Branch (1)

Office of the Chief of Ordnance
Department of the Army
The Pentagon
Washington 25, D. C.
Attn: Col. A. P. Tabor (ORDTB) (1)

Watertown Arsenal
Watertown 72, Massachusetts
Attn: Laboratory (1)

Office of Ordnance Research
Duke University
2127 Myrtle Drive
Durham, North Carolina
Attn: Dr. A. G. Guy (1)

AIR FORCES

U. S. Air Forces
Research and Development Division
The Pentagon
Washington 25, D. C. (1)

Air Material Command
Wright-Patterson Air Force Base
Dayton, Ohio
Attn: Materials Laboratory MCREXM (2)

Air Materiel Command
Wright-Patterson Air Force Base
Dayton, Ohio
Attn: Power Plant Laboratory (1)

Mr. Isaac Perlmatter
Met. Branch, Materials Lab.
Research Division
Wright-Patterson Air Force Base
Dayton, Ohio (1)

OTHER GOVERNMENT AGENCIES

U. S. Atomic Energy Commission
Division of Research
Metallurgical Branch
Washington 25, D. C. (1)

National Bureau of Standards
Washington 25, D. C.
Attn: Physical Metallurgy
Division (1)

National Advisory Committee
for Aeronautics
1724 F. Street, N. W.
Washington 25, D. C. (1)

Research and Development Board
Committee on Physical Sciences
The Pentagon
Washington 25, D. C.
Attn: Metallurgy Panel (1)

Oak Ridge National Labbratories
Oak Ridge, Tennessee
Attn: Metallurgical Division
Dr. Frye (1)

UNIVERSITIES

University of California
Department of Metallurgy
Berkeley, California
Attn: E. R. Parker (1)
J. E. Dorn (1)

Professor Pol Duwez
Department of Metallurgy
California Institute of Technology
Pasadena, California (1)

Professor R. F. Mehl
Metals Research Laboratory
Carnegie Institute of Technology
Pittsburgh, Pennsylvania (1)

Professor W. M. Baldwin
Metals Research Laboratory
Case Institute of Technology
Cleveland, Ohio (1)

The Johns Hopkins University
Applied Physics Laboratory
Silver Springs, Maryland
Attn: Dr. W. E. Gray (1)

Professor Robert Maddin
Department of Mechanical Engineering
The Johns Hopkins University
Baltimore 18, Maryland (1)

Massachusetts Institute of Technology
Department of Metallurgy
Cambridge, Massachusetts
Attn: Professor M. Cohen (1)
Professor N. J. Grant (1)

Massachusetts Institute of Technology
Project Meteor
Cambridge, Massachusetts
Attn: Guided Missiles Library
Room 22-001 (1)

Professor Paul A. Beck
Department of Metallurgical Eng.
University of Illinois
Urbana, Illinois (1)

Professor M. G. Fontana
Department of Metallurgy
University of Pennsylvania
Philadelphia, Pennsylvania (1)

Princeton University
Forrestal Research Center Library
Project SQUID
Princeton, University
Attn: M. H. Smith (1)

Rensselaer Polytechnic Institute
Department of Metallurgy
Troy, New York
Attn: Dr. W. F. Hess (1)

OTHER

Aerojet Engineering Corp.
Azusa, California
Via: Bureau of Aeronautics Rep.
15 S. Raymond Avenue
Pasadena, California (1)

Allegheny Ballistics Laboratory
Cumberland, Maryland (1)

S. J. Sindeband
American Electro Metal Corp.
320 Yonkers Avenue
Yonkers 2, New York (1)

Armour Research Foundation
Metals Research Laboratory
Technology Center
Chicago 16, Illinois
Attn: W. E. Mahin (1)

Battelle Memorial Institute
505 King Avenue
Columbus 1, Ohio
Attn: R. M. Parke (1)

Bendix Products Division
Bendix Aviation Corporation
401 Bendix Drive
South Bend 20, Indiana (1)

Dr. Max Gensamer
Department of Metallurgy
Columbia University
New York City (1)

Consolidated-Vultee Aircraft
Corporation
SanDiego, California
Via: Bureau of Aeronautics Rep.
Consolidated-Vultee
San Diego, California (1)

Dr. F. H. Driggs
Fansteel Metallurgical Company
North Chicago, Illinois (1)

General Electric Research Labs
Schenectady, New York
Attn: J. D. Nisbet (1)

M. W. Kellogg Company
Foot of Danforth Avenue
Jersey City 3, New Jersey
Attn: Special Projects Dept. (1)

Lukens Steel Company
Coatesville, Pennsylvania
Attn: T. T. Watson,
Director of Research (1)

Metallurgical Research & Development Co.
912 17th Street, N.W.
Washington, D. C. (1)

W. E. Kingston
Sylvania Electric Products, Inc.
Bayside, Long Island, New York (1)

Thompson Products, Inc.
2196 Clarkwood Road
Cleveland 3, Ohio
Attn: Director of Research (1)

Westinghouse Research Labs
Metallurgical Department
East Pittsburgh, Pennsylvania
Attn: Howard Scott (1)

Westinghouse Electric Corp.
Special Products Engineering
3 N. East Pittsburgh, Pennsylvania
Attn: Dr. W. H. Brandt (1)

Westinghouse Electric Company
Lamp Division, Research Laboratory
Bloomfield, New Jersey
Attn: Dr. J. W. Marden (1)

W. E. Shoupp
Westinghouse Electric Corporation
Atomic Power Division
Bettis Field
Pittsburgh, Pennsylvania (1)

OTHER

Dr. Wm. Blum
117 Chemistry Building
Bureau of Standards
Washington, D. C. (1)

Ryukiti Robert Hasiguti
Assistant Professor
Department of Metallurgy
University of Tokyo
Tokyo, Japan (1)

Mr. Alfred P. Ashton
Asst. Dir. I.C.R.
1315 St. Paul Street
Baltimore, Maryland (2)

Dr. I. R. Kramer
Horizons, Inc.
1215 H Street, N. W.
Washington, D. C. (1)